sustainability

MDPI

Article

Process Optimization for Sustainable Laser Powder Bed Fusion of Stainless Steel

Dionysios Markatos [1,*], Efthymios Polatidis [2], Sonia Malefaki [3], Christos Sofras [4,5] and Angelos Filippatos [1]

[1] Machine Design Laboratory, Department of Mechanical Engineering and Aeronautics, University of Patras, 26504 Patras, Greece
[2] Laboratory of Technology & Strength of Materials, Department of Mechanical Engineering and Aeronautics, University of Patras, 26504 Patras, Greece
[3] Department of Mechanical Engineering and Aeronautics, University of Patras, 26504 Patras, Greece
[4] Laboratory for Neutron Scattering and Imaging, Paul Scherrer Institut, Forschungsstrasse 111, 5232 Villigen, Switzerland
[5] Thermomechanical Metallurgy Laboratory (LMTM)—PX Group Chair, École Polytechnique Fédérale de Lausanne (EPFL), CH-2002 Neuchâtel, Switzerland
* Correspondence: dmark@upatras.gr

Abstract

Laser Powder Bed Fusion (L-PBF) enables the fabrication of complex components through layer-wise manufacturing, offering significant opportunities for improved material utilization and design flexibility. However, identifying sustainable process conditions remains challenging due to the trade-offs between manufacturing performance, environmental impact, economic cost, and social considerations. This study proposes a quantitative Sustainability Index (SI) framework for the integrated assessment and optimization of L-PBF process parameters. The proposed approach combines performance, environmental, and economic indicators into a single optimization objective, enabling sustainability to be directly incorporated into process parameter selection rather than evaluated only as a post-processing criterion. Social considerations are additionally incorporated through a context-dependent assessment to investigate the influence of geographical manufacturing conditions and stakeholder priorities. An experimental dataset comprising 154 L-PBF-manufactured 304L stainless steel specimens produced under different combinations of laser power, scanning speed, and hatch distance was employed to evaluate the proposed framework. Performance was assessed through density and crystallographic isotropy indicators, while environmental and economic aspects were quantified through operational energy consumption and manufacturing-related costs. Multi-Criteria Decision-Making was used to construct the SI, while a regression-tree-based surrogate model and differential evolution optimization algorithm were employed to identify sustainable processing conditions. The results demonstrate that improved sustainability performance is achieved through parameter combinations involving relatively low laser power, high scanning speed, and increased hatch distance, reducing energy consumption and operational costs while maintaining adequate material quality. The optimization procedure consistently identifies improved solutions under different weighting scenarios. Furthermore, the incorporation of country-specific social indicators reveals the influence of regional conditions and sustainability priorities on the final assessment outcomes. The proposed SI provides a quantitative decision-support framework for sustainability-oriented L-PBF optimization and establishes a transferable methodology for future sustainable additive manufacturing applications.

Academic Editors: Ersilia Cozzolino, Mosè Gallo and Iacopo Bianchi

Received: 29 September 2026
Revised: 11 November 2026
Accepted: 23 November 2026
Published: 27 November 2026

Copyright: © 2026 by the authors. Licensee MDPI, Basel, Switzerland. This article is an open access article distributed under the terms and conditions of the Creative Commons Attribution (CC BY) license.

Keywords: Laser Powder Bed Fusion (L-PBF); sustainability challenges; process parameter optimization; holistic sustainability framework; Sustainability Index; Multi-Criteria Decision Making (MCDM); austenitic stainless steel

1. Introduction

Metal Additive Manufacturing (AM), commonly known as Metal 3D printing, has significantly revolutionized the manufacturing landscape by enabling the production of intricate, complex-shaped components in a near-net-shape manner [1]. Among the various AM techniques, Laser Powder Bed Fusion (L-PBF) has emerged as a manufacturing process that drives innovation across numerous industries [2,3]. In L-PBF, a laser selectively melts successive layers of metallic powder distributed over a build platform, with the resulting material characteristics being strongly dependent on the selected process parameters [4–6].

Since the establishment of this manufacturing method, the research community focused on optimizing the parameters to establish a process window, aiming to minimize defects caused by excessive energy input (leading to keyhole porosity) or insufficient energy input (causing lack of fusion defects), which are the most profound challenges [5]. Simultaneously, the efforts aimed at suppressing or treating residual stresses [6], ensuring geometrical accuracy and mechanical integrity [7], or other aims at optimizing the productivity of the method [8]. After the establishment of process windows and the development of novel alloys and multimaterials, considerable efforts have been directed toward designing materials with unique microstructures that outperform conventional materials in both mechanical and functional properties [9,10]. To this end, recent implementations of machine-learning methods have facilitated the streamlining of the process optimization efforts [11].

Despite these technological advances, the sustainability of additive manufacturing processes has become an increasingly important research topic. Recent studies have highlighted the need to integrate sustainability considerations into the further development of L-PBF by accounting for the environmental, economic, and societal implications of the manufacturing process [12]. Sustainability is widely acknowledged as a multidimensional concept, typically framed through the three-pillar model that includes social, economic and environmental dimensions [13]. Nevertheless, the various dimensions of sustainability have frequently been examined in isolation, resulting in a wide range of interpretations and definitions over time. In recent years, the environmental aspect of sustainability has been at the forefront of both scientific inquiry and policy agendas [14].

Regarding metal AM techniques, particularly L-PBF, numerous recent studies have aimed to assess sustainability. A review of the current literature indicates that sustainability has been approached in varied manners, yet none has attempted to streamline the process parameters to improve sustainability. Works such as [15,16] demonstrate the use of Life Cycle Assessment (LCA) to assess sustainability by linking it to the environmental impact. In [15], LCA is employed to evaluate the environmental impact of additive manufacturing processes for alloys, focusing on parameters such as laser power (P), laser scanning speed (v), hatch distance (h), layer thickness (t) and energy density. In [16], eco-indicators are extracted to quantify sustainability in terms of environmental performance across various stages of the product lifecycle. These works highlight LCA's role in measuring environmental impacts based on both technical parameters and lifecycle considerations. Other works, such as [17,18], extend sustainability assessments by incorporating Life Cycle Cost (LCC) alongside LCA to account for cost aspects. Additionally, ref. [19]

introduces lead time as a critical factor in evaluating the sustainability of metal additive manufacturing.

To address the multidimensional nature of sustainability, several studies have incorporated multiple criteria through aggregated indicators and Multi-Criteria Decision-Making (MCDM) approaches. Studies such as [20,21], consider environmental, economic, and social criteria for evaluating additive manufacturing sustainability, while [22] introducing an aggregated indicator incorporating circular economy aspects. Furthermore, MCDM methodologies have been applied to compare additive manufacturing technologies and identify sustainable process alternatives based on combinations of material performance, machine characteristics, production costs, ecological impacts, and market-related factors [23–25]. Although these approaches provide valuable frameworks for sustainability evaluation, they mainly focus on assessing existing processes or comparing alternative technologies rather than directly optimizing manufacturing parameters, of a single manufacturing method, according to sustainability objectives.

In parallel, some studies have investigated the optimization of L-PBF process parameters considering individual sustainability-related aspects. For instance, ref. [26] optimized process conditions based on time and waste-related costs, while [27] focused on improving manufacturing efficiency by optimizing parameters such as layer height, build rate, and support structure requirements. Other studies have incorporated component performance into sustainability optimization by adjusting process parameters such as laser power, scanning speed, hatch distance, and layer thickness while considering criteria including surface roughness, tensile strength, elongation, and relative density [28]. Additional approaches have explored sustainability improvements through powder reuse strategies [29], defect reduction through parameter optimization [30], topology optimization for reduced environmental impact [31], and minimization of material losses and post-processing requirements [32]. Moreover, MCDM-based optimization approaches have been applied to identify favorable combinations of L-PBF parameters by simultaneously considering multiple performance indicators [33].

These studies demonstrate that sustainability in additive manufacturing is evaluated through diverse combinations of environmental, economic, social, and performance indicators. However, the absence of a unified quantitative metric limits the direct integration of sustainability objectives into L-PBF parameter optimization. In particular, existing approaches rarely consider sustainability as an explicit optimization objective while simultaneously accounting for process performance, environmental impact, economic aspects, and contextual social factors.

To address this challenge, the present study proposes a sustainability-driven optimization framework for L-PBF based on the development of a quantitative Sustainability Index (SI). The proposed SI integrates performance, environmental, and economic indicators into a single metric that can be directly employed as an optimization objective for process parameter selection. The novelty of the approach lies in linking process parameters not only to environmental and economic performance, but also to the resulting part quality through density and crystallographic isotropy, thereby explicitly accounting for process–quality trade-offs in sustainability optimization. In addition, social considerations are incorporated through a context-dependent assessment to investigate the influence of geographical manufacturing conditions and stakeholder priorities on sustainability outcomes. The SI was formulated based on the synthesis of the authors' previous research contributions (Section 2.2) and it is applied to optimize key L-PBF parameters, including laser power, scanning speed, and hatch distance.

The proposed methodology is experimentally evaluated using L-PBF-manufactured austenitic stainless-steel specimens produced under systematically varied processing conditions. Regression modelling, MCDM, and evolutionary optimization algorithms are

combined to identify sustainable processing conditions. The results demonstrate the capability of the proposed SI to provide a quantitative decision-support framework for sustainability-oriented L-PBF optimization and establish a transferable methodology for future sustainable additive manufacturing applications.

2. Materials and Methods

2.1. Experimental Dataset

The process-parameter combinations employed in the present study were chosen based on prior understanding of their influence on crystallographic texture development [34,35], where a systematic exploration of the L-PBF parameter space was conducted to establish an optimized processing window for tailoring crystallographic texture evolution. In the current study, this experimentally derived parameter space is leveraged to investigate the influence of manufacturing conditions on sustainability performance. While these processing conditions provide a means to tailor the resulting microstructures, their implications from a sustainability perspective have not been previously addressed and constitute the focus of the present work.

The manufacturing process was undertaken at the Swiss Federal Laboratories for Materials Science and Technology, EMPA, Switzerland using a Sisma MySint 100 machine. The dataset was produced from a series of samples of 5 × 5 × 5 mm^3 from 304L stainless steel with process parameter variations: laser power (W) 110–120–135–150–160–175, laser scanning speed (mm/s) 400–600–800–1000–1200–1400, and hatch distance (μm) 60–70–80–90–100 using a bidirectional scanning strategy without any rotation between the successive layers. The bidirectional scanning strategy without interlayer rotation is suitable for the present investigation, as it allows the influence of processing parameters on crystallographic texture to be assessed while maintaining a consistent basis for evaluating sustainability metrics. The layer thickness was kept constant to 30 μm for all samples. Although the selected parameter levels correspond to 180 possible combinations in a full factorial design, combinations associated with excessively high volumetric energy density (VED) were deliberately excluded based on prior processing experience. This selection aimed to minimise the risk of severe defect formation and process instabilities that could jeopardise the entire build job, resulting in 154 specimens for the present analysis.

The sample quality metrics include density, determined by the Archimedes method for all specimens, thereby directly capturing the effect of the broad process-parameter range on consolidation. Moreover, it is well known that under a specific range of process parameters, strongly anisotropic material properties are obtained due to the development of strong crystallographic texture [34]. In these cases, strong <110>- and/or strong <100>-crystallographic texture builds along the building direction (BD). Therefore, instead of mechanical characterization by tensile testing along an arbitrary direction, the mechanical anisotropy was assessed through the crystallographic texture. The texture data were obtained by time-of-flight neutron diffraction using the POLDI diffractometer at the SINQ neutron source, Paul Scherrer Institute (PSI), Switzerland. Measurements were performed using a 3.8 × 3.8 × 3.8 mm^3 gauge volume, with the samples oriented such that the scattering vector was parallel to the BD. Texture along each direction was assessed from the relative integrated intensities of the 200 and 220 reflections, normalized by the summed intensities of the 111, 200, 220, and 311 fcc reflections. Further details of the experimental procedure and data analysis are provided in [34]. As such, by ensuring a dense structure and a high degree of crystallographic isotropy (i.e., absence of crystallographic texture), the material exhibits uniform mechanical properties, closely matching the nominal values for strength and ductility in all directions as shown in [34]. In contrast, strongly anisotropic samples can exhibit a wider range of mechanical properties, i.e., yield strength, ultimate tensile strength, ductility, etc., depending on the loading direction (under uniaxial

tension/compression) or more complex stress states applied. Accordingly, materials characterized by strong mechanical anisotropy are not considered suitable within the scope of the present study. Nevertheless, density and crystallographic isotropy do not capture all aspects of mechanical performance, and future extension of the framework should incorporate mechanical characterization along multiple loading directions. To quantify crystallographic anisotropy from neutron diffraction, the relative texture intensities for the 220 and 200 diffraction peaks, respectively, compared to other orientations, were considered.

The anisotropy index (AI) was defined as follows:

$$AI = |I_{220} - 0.29| + |I_{200} - 0.33| \quad (1)$$

where I_{220} and I_{200} represent the integrated intensity of the corresponding reflection, relative to other diffraction peaks. The reference values 0.29 and 0.33 correspond to the expected I_{220} and I_{200} of a randomly textured polycrystalline material respectively. These values were experimentally determined from the raw L-PBF powder of the same material measured in a capillary and represent the corresponding relative intensities for a randomly oriented reference sample, i.e., a powder measurement. Thus, an AI value of zero indicates a perfectly isotropic material, while higher values reflect increasing anisotropy. Since AI does not range between 0 and 1, a Normalized Isotropy Index (NII) was introduced to allow direct comparison across samples:

$$NII = 1 - \frac{AI - min(AI)}{max(AI) - min(AI)} \quad (2)$$

where $max(AI)$ and $min(AI)$ the maximum and the minimum of the AI amongst the samples respectively. By construction, NII approaches 1 for nearly isotropic samples and decreases toward 0 with increasing crystallographic anisotropy. This isotropy index is employed in the following sections to evaluate the influence of processing parameters on crystallographic texture development and, together with density, serves as a criterion for assessing the performance of the manufactured samples. This approach enables rapid and resource-efficient performance assessment of 154 samples, minimising the need for large-scale specimen fabrication, tensile testing, and time-consuming EBSD measurements to characterise crystallographic texture and assess directional properties along multiple directions. For completeness, the density and crystallographic isotropy results for all 154 specimens are provided as Supplementary Material, allowing a comprehensive overview of the measured quality characteristics across the investigated process-parameter combinations.

2.2. A Holistic Index to Assess L-PBF Sustainability

The holistic SI presented in Equation (3), originally developed and applied at the process level in [36], is herein extended with targeted modifications to assess the sustainability performance of the fabricated samples and capture the trade-offs associated with the manufacturing process. Consequently, the following integrated index is formulated as the principal design criterion for an assessed engineering component or product, represented in the present study by the fabricated samples.

$$SI = w_P \times P' + w_E \times E' + w_C \times C' + w_{SOC} \times SOC' \quad (3)$$

where $\sum_j w_j = 1$, $j \in \{P', E', C', SOC'\}$.

In the above equation, P'represents the performance indicator. In this study, performance is defined in terms of material density, acknowledged as the primary quality indicator for components produced via additive manufacturing, along with mechanical isotropy, as outlined above. Consequently, P' is obtained by averaging the NII (see Equation (2)) and the normalized density, d'. Moreover, E', C' and SOC' correspond to the normalized indicators of environmental impact (E), cost competitiveness (C), and social

conditions (SOC) in the manufacturing country, respectively. The normalization of data constitutes a fundamental step in the MCDM process, as it brings heterogeneous criteria onto a common scale, which allows meaningful comparison. There exist several normalization methods in the literature, such as Min-Max (or linear) method, z-score method, vector method and others [36]. In the current study, Min-Max normalization is adopted as it preserves the relative differences and scales all criteria to a common range between 0 and 1. In this case, the normalized value x′ of x is given by:

$$x' = \frac{x - min(x)}{max(x) - min(x)} \quad (4)$$

for the attribute that needs to be maximized (for sample density, d) and

$$x' = 1 - \frac{x - min(x)}{max(x) - min(x)} \quad (5)$$

for the attributed that needs to be minimized (for E, C and SOC), where min and max are the minimum and the maximum values of the corresponding indicator respectively.

The choice of normalization method is further supported by the comparative analysis of MCDA methods and normalization techniques conducted by Malefaki et al. (2025) [37], which emphasizes the importance of selecting an appropriate normalization approach according to the specific application and identifies favorable robustness characteristics for the combination of the weighted sum method and min–max normalization in a comparable case study.

Moreover, w_P, w_E, w_C, and w_{SOC} are the weight factors of P', E', C' and SOC' respectively that reflect the importance of the corresponding attribute on the holistic index. For the determination of the criteria weights, the Analytical Hierarchy Process (AHP) method was used [38]. The holistic SI is defined on a normalized scale ranging from 0 to 1. The final ranking of all the available components is based on the value of the SI.

Since the study employs a single material from the same supplier and processes it on the same machine, the influence of material and equipment variations is considered constant across all samples and therefore ruled out from the comparative assessment. As all specimens were manufactured simultaneously, energy and argon consumption were allocated to individual specimens according to their respective processing times. Argon consumption was estimated assuming a constant supply rate of 0.3 L/min (at 0.2% O_2 level, as per manufacturer), while cooling-system energy consumption was calculated assuming a constant power demand of 1750 W. Laser-related electrical energy consumption was calculated from the applied laser power and processing time, assuming an electrical-to-optical efficiency of 26.7% for the fibre laser, corresponding to an electrical input-to-optical output conversion factor of 3.75 [39]. Thus, variations in laser power and processing time arising from the different process parameters were directly reflected in the calculated laser-related energy consumption.

The environmental impact is expressed as a function of the total energy consumption (kWh) required fabricating each sample, multiplied by an emission factor (40.0 gr CO_2 per kWh) specific to the manufacturing location (Switzerland in this case). Finally, costs are expressed as the total energy consumption per sample, converted to kWh, multiplied by the cost of electricity (0.34 €/kWh), plus the consumption of inert gas (argon) per sample, multiplied by the corresponding cost (0.03 €/L). The total energy consumption includes both the energy expended by the laser during operation and that consumed by the L-PBF machine's cooling system throughout the process.

In the preliminary stage of the assessment, the sustainability of the produced samples is examined using the available dataset, according to the SI pillars presented above. This step provides a baseline understanding of the sustainability profile across the samples. Following this, the L-PBF parameters are optimized with the goal of improving the sustainability performance by targeting the identified key indicators. Social considerations

are not addressed during the initial assessment, since all cubes are produced in the same laboratory. Instead, these factors are integrated into a subsequent, more comprehensive evaluation. The secondary assessment, described in Section 2.4, extends the analysis by incorporating social indicators, thereby enabling a more holistic evaluation of sustainability consistent with its multidimensional nature. To investigate the influence of stakeholder priorities across the sustainability pillars, three weighting scenarios were examined. These include an equal-weighting scenario for all pillars of the holistic SI, a cost-oriented scenario, and an environmentally oriented scenario. This scenario-based approach enables a comparative assessment of how alternative weighting priorities affect the holistic SI and the identification of optimal operating conditions. The corresponding weighting factors were derived using the AHP.

2.3. Optimization of Process Parameters for Enhanced Sustainability in L-PBF

One of the main goals of the current work is to optimize the SI with respect to the laser power, laser scanning speed and hatch distance. The objective function, SI, depends indirectly on the process parameters through the performance, which is a function of density and mechanical isotropy, as well as through environmental and cost factors.

Regression Tree (RT) models [40,41] were employed to predict both density and the crystallographic isotropy index as functions of the process parameters. In addition to the three individual process parameters, the areal energy density (AED = LP/(SP · HD)) was included as a derived predictor to account for their combined effect on the process response. Although energy density is a widely used descriptor of the process conditions in laser powder bed fusion, it does not fully capture the effects of different parameter combinations on melt pool characteristics and defect formation [42,43]. Therefore, it was included alongside the individual process parameters. The developed models were then used to estimate both performance indicators for parameter combinations beyond those directly represented in the experimental dataset, and the resulting predictions were considered in the optimization procedure. To improve model generalizability and reduce overfitting, cost-complexity pruning was applied. The pruning process was governed by the complexity parameter (cp), which specifies the minimum error reduction required to retain a split. The optimal model configuration was determined through parameter tuning and subsequently adopted for analysis.

The predictive performance of the linear regression and RT models was evaluated using repeated 10-fold cross-validation with 30 random partitions of the 154 observations. Both models included laser power, scanning speed, hatch distance, and areal energy density as predictors. In each repetition, the models were trained on nine folds and evaluated on the remaining fold, ensuring that each observation was predicted by a model that had not been trained on it. Both models were evaluated using identical data partitions.

Regression trees were fitted using the rpart package in R, with the ANOVA splitting criterion, a minimum splitting node size of 20, a minimum terminal node size of 7, and an initial complexity parameter of 0.0001. Tree pruning was performed within each training fold by selecting the complexity parameter that minimized the internal 10-fold cross-validation error, following a nested cross-validation approach. Table 1 reports the in-sample and cross-validated mean squared errors (MSE), root mean squared errors (RMSE), and cross-validated coefficients of determination (CV R^2). As expected, in-sample errors were lower than cross-validated errors, particularly for RTs, highlighting the importance of cross-validation when comparing models with different levels of flexibility. The RTs achieved lower cross-validated MSE than linear regression for both density (0.0372 vs. 0.0414) and anisotropy index (0.0120 vs. 0.0135), corresponding to reductions of approximately 10% and 11%, respectively. Although these repetitions are not statistically independent, the results indicate a consistent, albeit modest, predictive advantage of the RT.

Table 1. In-sample and cross-validated (10-fold, 30 repetitions) prediction errors of the linear regression and regression tree models.

Response	Model	In-Sample MSE	CV MSE	CV RMSE	CV R^2
Density	Linear regression	0.0375	0.0414	0.203	0.29
Density	Regression tree	0.0330	0.0372	0.193	0.36
Anisotropy index	Linear regression	0.0127	0.0135	0.116	0.38
Anisotropy index	Regression tree	0.0066	0.0120	0.110	0.45

In addition to improved accuracy, the RT approach provides an interpretable representation of the relationships between process parameters and density, highlighting its suitability for additive manufacturing applications.

The weighted SI was subsequently evaluated for all combinations of laser power, scanning speed, and hatch distance. To identify the process-parameter triplet that maximizes the SI, a differential evolution (DE) optimization algorithm [40] was employed. Conventional gradient-based optimization methods, such as BFGS, were not suitable in this case due to the non-differentiable nature of the objective function and the absence of reliable gradient information. DE is a population-based global optimization algorithm that iteratively evolves candidate solutions through mutation, crossover, and selection operations. Owing to its robustness and derivative-free formulation, DE is particularly well suited for navigating complex and potentially non-convex search spaces. The optimal process parameters were therefore determined using the DE algorithm.

The aforementioned approach was implemented in the R language (ver. 4.3.1) [44]. More specifically, for the RT estimation, the "rpart" library [45] was used and the "DEoptim" library was used for the maximization of the SI objective function with respect to laser power, laser scanning speed and hatch distance.

2.4. Context-Dependent Assessment of Social Sustainability Indicators

To address the social dimension of sustainability, a structured assessment was performed through a hypothetical scenario in which production samples were manufactured in different countries, employing the same raw material and the same AM machine. This scenario includes eight countries, i.e., four from Europe, two from Asia and two from the Americas, which are chosen as indicative examples. The aim is to gain insights into regional differences in social impact, which plays a critical role in the overall SI assessment of the manufacturing process. This approach underscores the importance of considering location-specific factors in sustainability assessments, promoting transparency and encouraging the manufacturing sector to make informed decisions that balance profit, environmental responsibility and social equity. The assessment uses the UNEP/SETAC Social Life Cycle Assessment (SLCA) framework [45], a comprehensive approach that evaluates social impacts through multiple stakeholder perspectives. Using the ANSYS SLCA tool [46], which provides streamlined assessments across social impact categories, specific social impact categories linked to various stakeholders are identified including workers, consumers, local communities and society at large. The data sources for the selected social indicators are documented within the SIAT tool. For each country, a detailed evaluation of normalized (0–100) social impact metrics, such as labor conditions, fair wages and community well-being, is performed. Indicators with missing data are excluded from the assessment and are not considered in the corresponding calculations. To derive the social impact index, the average of twenty-six normalized metrics is calculated, resulting in an aggregated social index attributed to each country considered. The normalized social impact index serves as an essential component of the holistic SI and it was integrated into the calculation of the SI as defined in Equation1. The remaining pillars of performance, environment and costs are calculated based on the optimized process parameters, which are consistent across all countries and are obtained

from the optimization procedure described in Section 2.3. To account for differences between countries, environmental emissions are adjusted using the emission factor specific to the country of manufacturing [47]. To ensure accurate cost representation, manufacturing costs in each country are adjusted based on local non-household electricity prices [48–55], reflecting the varying energy expenses that contribute to production costs. Additionally, labor costs are incorporated for a more comprehensive assessment of total production expenses [56–59]. With this comprehensive data, a ranking of the nine countries is performed, based on their SI scores. To account for diverse priorities among the four sustainability pillars: performance, environment, costs and society, three distinct weighting scenarios are considered. In the first scenario, equal weights are assigned to all pillars. The second scenario prioritizes environment and society over performance and costs, while the third scenario prioritizes performance and costs over environment and society.

It should be noted that although the aggregated national indicators provide an indicative assessment, they cannot directly represent the actual social performance of individual manufacturing facilities, companies or supply chains, as they do not capture company-specific practices or local working conditions. Therefore, the results should be interpreted as a preliminary screening of potential social sustainability differences rather than a direct measurement of manufacturing-level social impacts.

3. Results and Discussion

3.1. Ranking of Samples Based on Sustainability Index

Table 2 summarizes the top five process parameter configurations yielding the highest sustainability performance for the printed samples, each associated with a distinct ID and SI. The evaluation covers three scenarios: (a) equal weighting among the pillars of performance, environmental impact and costs; (b) prioritizing environmental impact; and (c) prioritizing cost efficiency.

Table 2. Ranking samples based on their SI, LP: laser power; SP: scanning speed; HD: hatch distance; SI: Sustainability Index.

SI—Equal Weights		
[LP, SP, HD]	**SI**	**Configuration ID No**
[120, 1400, 90]	0.9313	135
[175, 1400, 100]	0.9274	128
[160, 1400, 90]	0.9271	100
[160, 1200, 100]	0.9239	104
[160, 1400, 100]	0.92244	105
SI—priority to environment		
[LP, SP, HD]	**SI**	**Configuration ID No**
[120, 1400, 100]	0.9647	129
[150, 1400, 100]	0.9560	81
[160, 1400, 100]	0.9549	105
[175, 1400, 100]	0.9532	128
[120, 1400, 90]	0.9522	135
SI—priority to costs		
[LP, SP, HD]	**SI**	**Configuration ID No**
[175, 1400, 100]	0.9693	128
[160, 1400, 100]	0.9673	105
[120, 1400, 100]	0.9672	129
[150, 1400, 100]	0.9659	81
[120, 1400, 90]	0.9550	135

A key observation is that most of the top-ranked combinations consistently appear in the first five places across all scenarios, demonstrating stability in their sustainability ranking regardless of the scenario. The findings indicate that components fabricated with process parameters that are characterized by relatively low laser power, elevated scanning speed and increased hatch distance, exhibit superior performance from a sustainability point of view (sample 129). This is justified by the interplay of these parameters in maximizing productivity, or minimizing resource consumption and energy usage, while avoiding the formation of porosity and high mechanical anisotropy. Low laser power reduces energy consumption, which not only minimizes environmental impact but also lowers operational costs. High scanning speed decreases production time, resulting in additional cost savings while reducing the total energy required for manufacturing. A larger hatch distance reduces laser overlap, which optimizes laser power usage. Moreover, the similarity in SI values among the top-performing combinations indicates that they exhibit comparable levels of sustainability, thereby allowing for greater flexibility in selecting process parameters, to achieve specific mechanical anisotropy, without significantly affecting the overall sustainability outcome.

The violin charts in Figures 1–3 illustrate the distribution of SI across the process parameters (laser power, scanning speed and hatch distance) by combining a boxplot with a kernel density estimate. This visualization provides detailed insights into both the central tendency and the variation in the SI values, while also revealing potential asymmetries in the data. For reasons of space, the illustrated results correspond to the scenario where the sustainability pillars, performance, environment and cost, are equally prioritized, see Table 1, SI-equal weights. On the y-axis, the SI is depicted, while the x-axis illustrates the process parameters; and for each parameter value a violin exists. The shape of each violin provides insights into the density of sustainability values; wider sections indicate a higher frequency of scores in that range, while narrower sections suggest fewer data points. The central features include markers for the median and interquartile range, while the outer shape shows the distribution's spread and variability, as in a density plot. Specifically, when examining the impact of laser power on the SI (Figure 1), no distinct or consistent trend can be observed. This suggests that the relationship between laser power and sustainability is complex and potentially influenced by other interacting process parameters. Regarding the scanning speed (Figure 2), it is evident that the SI increases exponentially as the scanning speed rises. This underscores the pivotal importance of scanning speed in the manufacturing process, as it directly influences sustainability. Finally, sustainability appears to increase linearly with hatch distance (Figure 3), highlighting the significance of optimizing this parameter to achieve improved sustainability outcomes. Together, these findings emphasize that carefully calibrating the interplay of laser power, scanning speed and hatch distance, is crucial for achieving an optimal balance across the environmental, economic and performance dimensions of sustainability. Meanwhile, the exponential relationship between scanning speed and SI highlights the importance of maximizing efficiency without compromising the quality of the output, thereby reducing time and energy usage while maintaining precision. Additionally, the linear improvement in sustainability with increasing the hatch distance suggests that larger distances between hatch lines can contribute to improved energy efficiency, potentially reducing the environmental footprint of the process. This holistic understanding underscores the importance of a data-driven approach to parameter optimization, ensuring that all three aspects, i.e., environmental impact, economic viability and operational performance are aligned to support more sustainable manufacturing practices.

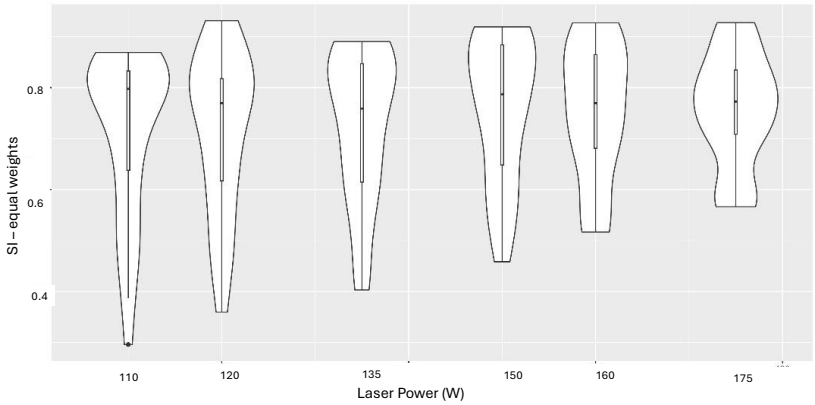


Figure 1. Violin plot of the Sustainability Index distribution for different laser power values.

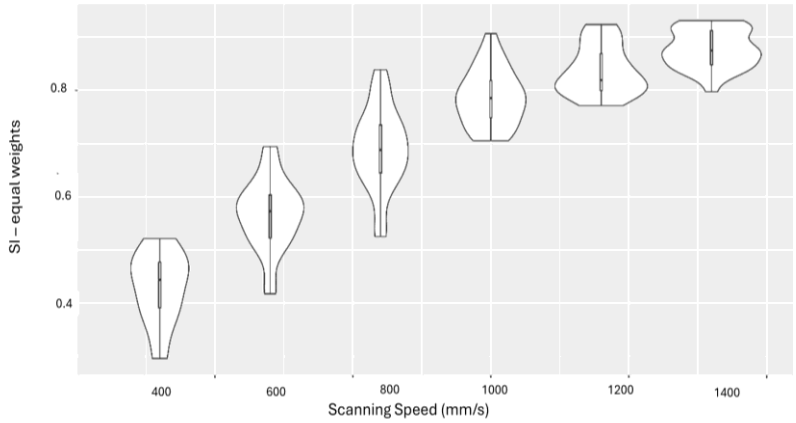


Figure 2. Violin plot of the Sustainability Index distribution for different scanning speed values.

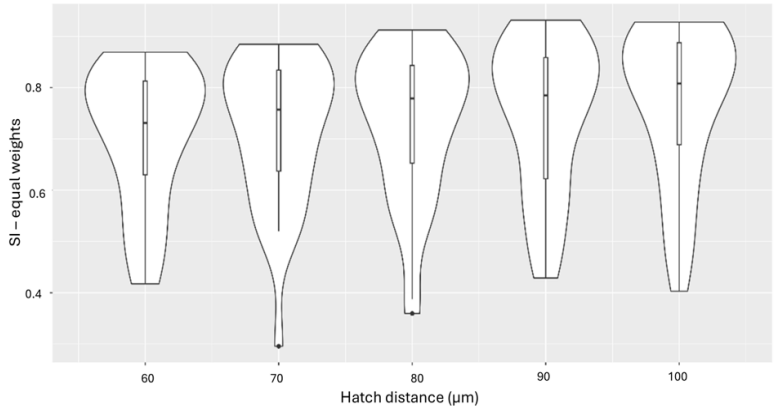


Figure 3. Violin plot of the Sustainability Index distribution for different hatch distance values.

3.2. Process Optimization for Enhanced Sustainability

Table 3 illustrates the predicted optimal process parameters that were determined for each of the three different scenarios: equal weighting of sustainability pillars, prioritization of environmental considerations, and prioritization of cost efficiency. Additionally, Table 3 presents the corresponding values obtained for each of the three sustainability pillars, i.e., performance, environmental, cost, as well as the resulting SI calculated for each scenario. Comparing the optimized results with those from the experimental dataset (Table 2) shows that the optimization led to modest improvements in the SI. These gains reflect fine-tuning within the existing parameter space rather than a major shift, indicating

incremental but meaningful progress in sustainability performance. Among the three scenarios, it is commonly observed that maximizing scanning speed and hatch distance ensures high productivity, while incorporating moderate values of laser power helps maintain adequate density. The similar outcomes obtained for the environmental-priority and cost-priority scenarios can be partly explained by the shared dependence of the corresponding indicators on energy consumption. This dependence may result in overlapping contributions to the SI. Nevertheless, the two indicators capture different sustainability aspects and are therefore maintained separately in the proposed assessment framework. The identified optimal parameter combinations are model-derived and have not been experimentally validated; they should therefore be regarded as predicted processing conditions requiring further experimental validation. Nevertheless, similar optimization approach has shown good agreement between predicted and experimentally validated outcomes in terms of isotropy/anisotropy in [34].

Table 3. Optimal process parameters for different SI scenarios.

Scenario	Optimal Process Parameters			Sustainability Pillars and SI			
	Laser Power	Scanning Speed	Hatch Distance	P (Weight)	E (Weight)	C (Weight)	SI
SI-Equal weights	127.5	1400	95	0.8567 (0.33)	0.0211 (0.33)	0.0133 (0.33)	0.9408
SI-Environmental impact prioritized	127.5	1400	100	0.7941 (0.14)	0.0076 (0.72)	0.0001 (0.14)	0.9657
SI-Cost competitiveness prioritized	127.5	1400	100	0.7941 (0.14)	0.0076 (0.14)	0.0001 (0.72)	0.9700

3.3. Sustainability Assessment Including Social Aspects

Table 4 presents the normalized social impact metrics (0–100) for the countries considered for manufacturing. Based on these metrics and the methodology detailed in Section 2, the SI incorporating social aspects is calculated, accounting for the three different scenarios. In these calculations, the optimal combinations of process parameters are applied for each scenario (cf. Table 3). The results show that incorporating country-specific electricity prices does not significantly affect the final index, as overall costs are predominantly determined by raw material and resource expenses.

In the first scenario, where equal weighting is applied to the four sustainability pillars, the highest sustainability scores are achieved by Norway, followed closely by Switzerland. China scores the lowest in this scenario. This can be attributed to Norway and Switzerland's strong social and environmental policies, which help maintain a high SI. China, on the other hand, shows relatively lower performance in social impact and environmental sustainability metrics, which affects its overall score when all sustainability pillars are weighted equally.

Table 4. Social Impact metrics (normalized) for the countries under consideration; **CHE**: Switzerland; **NOR**: Norway; **CZE**: Czech Republic; **GRC**: Greece; **CHN**: China; **UAE**: United Arab Emirates; **USA**: United States of America; **CAN**: Canada.

	Countries	CHE	NOR	CZE	GRC	CHN	UAE	USA	CAN
Workers	Child labor	100	100	100	100	100	100	100	100
	Forced labor& slavery	64	63	54	37	55	64	69	89
	Minimum wage	n/a	n/a	23	33	7	n/a	53	74

Consumers	Hours worked per week	61	85	71	71	71	24	71	71
	Women's share of labor force	83	86	77	76	78	19	82	83
	Fatal accidents at work	98	98	92	98	80	85	93	93
	Social protection expenditure	93	94	80	84	62	77	89	85
	ITUC freedom of association	80	100	n/a	41	21	21	41	60
	Press freedom	95	100	79	73	10	54	83	89
	Rule of law	98	100	83	63	53	79	88	93
	Corruption perception index	95	95	60	49	41	78	88	91
	Recycle rate	80	63	32	29	n/a	n/a	54	38
Local Community	Political freedom and civil rights	100	100	100	84	18	18	100	100
	Total literacy	88	86	69	66	58	77	85	79
	Wellbeing, satisfaction with life	95	97	68	61	38	89	88	98
	Voice and accountability	99	100	79	79	5	16	73	96
	Political stability	93	94	79	51	38	66	46	90
	Unemployment rates	85	86	92	57	87	91	85	79
Society	Ecological Footprint	72	64	67	75	79	40	49	51
	UN Human Development Index	100	100	90	88	66	88	95	95
	R&D spend	60	35	36	26	44	27	62	28
	Global Peace Index	87	83	87	63	55	71	51	87
	Control of corruption	97	98	71	59	53	83	83	92
	Regulatory quality	94	96	87	72	50	83	88	94
Value	Good Country Index	92	94	84	79	60	62	73	97
	IP protection	89	n/a	n/a	n/a	32	33	100	57
	SI (equal weights)	0.8251	**0.8531**	0.8251	0.7747	0.7019	0.7277	0.7954	0.8430
	SI (prioritize environment & performance)	0.9046	**0.9203**	0.8079	0.7247	0.5947	0.6723	0.8128	0.8683
	SI (prioritize cost competitiveness and performance)	0.7368	0.7810	**0.8657**	0.8589	**0.8625**	0.8191	0.7897	0.8268

In the second scenario, where environmental and performance factors are prioritized over costs and social impact, Norway again achieves the highest sustainability score, with Switzerland following closely behind. China obtains the lowest SI value. This outcome reflects the environmental policies and high performance in sectors such as energy efficiency and innovation in Norway and Switzerland, which allow them to excel when these pillars are prioritised. China has made substantial progress across several domains;

however, like many countries, it continues to address ongoing environmental and social challenges, which are reflected in its positioning within this scenario.

In the third scenario, where performance and costs are prioritized over environmental and social factors, China and the Czech Republic achieve almost the same highest sustainability scores. Switzerland ranks the lowest in this scenario. The results indicate that Czech Republic and China are more competitive when performance and cost efficiency are the key priorities, as both countries have lower operational costs and strong manufacturing performance. However, Switzerland's focus on high environmental and social standards, together with high labour cost, results in a lower score in this scenario, as these factors are less emphasized compared to performance and cost. The differences in these rankings highlight the varying strengths and challenges that each country faces, as they prioritize specific aspects of sustainability based on their economic models, policy frameworks and regional contexts. When accounting for social considerations, European countries generally present more favourable sustainability scores compared to those outside Europe.

An important point to note is that Social Impact Assessment Tool- (SIAT-) based indicators, such as forced labour and slavery, may have scores below 50 for certain countries. These scores are interpreted relative to the global average, with 50 representing the global average and lower values indicating levels below this benchmark. The indicators support the identification of potential social risks in global supply chains. However, they reflect country-level conditions and do not constitute direct evidence of the presence or absence of such practices in a specific company or product. Instead, they provide insight into the broader social context and potential exposure to risks associated with production and supply-chain activities.

Furthermore, the social sustainability assessment relies on aggregated country-level indicators and should therefore be interpreted as a preliminary screening of potential social risks, rather than a direct assessment of specific manufacturing facilities or supply chains. Where data were unavailable for certain national indicators, these entries were retained as n/a without imputing values. This may affect the completeness of cross-country comparisons. Future work should incorporate more detailed, facility- and supply-chain-specific social data to strengthen the assessment.

3.4. Comparison with Relevant Literature

The main contribution of the present work is the integration of part quality, environmental impact, cost, and social indicators into a unified framework for L-PBF process-parameter optimization, enabling alternative parameter configurations to be evaluated under different sustainability priorities.

Multiple previous studies have investigated the relationships between L-PBF processing conditions, part quality, and manufacturing performance. For instance, Diaz Vallejo et al. [60] demonstrated that density in L-PBF-produced stainless steel 316L is affected by process parameters, including laser power, scanning speed, and hatch distance, with unsuitable processing conditions potentially leading to porosity. Similarly, Evangelou et al. [61] showed that density and microstructural characteristics are influenced by process parameters and scanning strategy. Consistent with the importance of these parameters in determining part quality, the present optimization identifies a scanning speed of 1400 mm/s, a hatch distance of 95–100 μm, and a laser power of 127.5 W as favourable settings under the adopted performance criteria. However, the present study extends the scope of these investigations by evaluating process configurations not only in terms of technical performance but also in terms of their environmental, economic, and social implications. Furthermore, the relatively large hatch distances selected by the optimization should be interpreted in the context of the other process parameters and the specific parameter range investigated, as their effect on density cannot be generalized across different L-PBF configurations.

https://doi.org/10.3390/su182312142

Crystallographic characteristics are another important consideration in L-PBF process optimization. Sofras et al. [9] investigated crystallographic texture in L-PBF-produced 304L stainless steel and demonstrated that scanning speed and hatch distance influence crystallographic texture in different build directions. This finding supports the consideration of crystallographic isotropy alongside density in the present framework. While Sofras et al. [9] focused on understanding and predicting processing conditions that promote strong crystallographic texture and anisotropy, the present study incorporates crystallographic isotropy into a broader optimization framework that also considers environmental, economic, and social performance. Although isotropy or anisotropy may be desirable depending on the intended application, isotropy is adopted here as a baseline performance criterion, reflecting the preference for uniform, direction-independent mechanical properties. Thus, the selected process parameters are evaluated against a wider set of objectives, although the extent to which the optimized configurations improve isotropy must be established from the corresponding results of the present study. The importance of considering environmental and economic performance alongside technical quality is also highlighted by previous sustainability studies. Liao et al. [18] assessed the environmental impacts of L-PBF and conventional manufacturing using a parametric model, demonstrating the relevance of manufacturing settings, part characteristics, and production conditions to environmental performance. Their work complements the present study: while Liao et al. [18] focused on modelling and comparing environmental impacts, the present framework incorporates environmental impact into the multi-criteria optimization of L-PBF process parameters, together with technical, economic, and social indicators. Similarly, Rizk et al. [62] compared L-PBF and conventional machining for Ti-6Al-4V using a multi-criteria sustainability assessment. Whereas their study evaluates the relative sustainability of alternative manufacturing processes, the present study identifies L-PBF parameter configurations that perform favourably under different sustainability priorities.

4. Concluding Remarks

This study develops and experimentally evaluates a sustainability-driven optimization framework for L-PBF based on a quantitative SI. The proposed methodology integrates performance, environmental, and economic indicators into a single optimization criterion, enabling sustainability considerations to be directly incorporated into L-PBF process parameter selection rather than evaluated only as a post-processing assessment. In addition, a context-dependent social sustainability assessment was introduced to investigate the influence of manufacturing location and stakeholder priorities on the overall sustainability outcome.

The framework is demonstrated using an experimental dataset comprising 154 LPBF-manufactured 304L stainless steel specimens produced under systematically varied combinations of laser power, scanning speed, and hatch distance. Component performance is assessed through density and crystallographic isotropy indicators, while environmental and economic aspects are quantified through operational energy consumption and manufacturing-related costs. The results demonstrate that the proposed SI can effectively capture the trade-offs between competing sustainability criteria and provide a quantitative basis for identifying favorable L-PBF processing conditions.

Across different weighting scenarios, the highest sustainability scores were consistently obtained at 127.5 W laser power and 1400 mm/s scanning speed, with an optimal hatch distance of 95–100 μm (Table 3). These values correspond to an intermediate-low laser power, the upper limit of the investigated scanning-speed range, and the upper end of the investigated hatch-distance range, respectively. While these parameters generally reduce processing time, energy consumption and cost, their contribution to the SI is simultaneously balanced against the resulting part performance through density and

crystallographic isotropy. Thus, the identified optimum does not simply reflect maximum manufacturing efficiency but represents a balance between resource efficiency and part quality within the investigated process window. The optimization procedure further improves the sustainability performance compared with the experimentally evaluated configurations, demonstrating the capability of the proposed framework to identify enhanced process conditions beyond direct evaluation of the available dataset. The incorporation of social sustainability indicators through a location-dependent assessment demonstrates that sustainability outcomes are influenced not only by manufacturing parameters but also by geographical and socioeconomic conditions. The ranking of manufacturing scenarios varied according to the selected weighting strategy, highlighting the importance of considering stakeholder priorities when evaluating sustainable production pathways.

In summary, the proposed framework advances sustainability assessment in additive manufacturing by jointly considering performance, economic, environmental, and social dimensions. The results demonstrate the feasibility of incorporating multidimensional sustainability criteria into process-parameter optimization and decision-making. Nevertheless, the scope of the present study was restricted to a single material and manufacturing configuration. Future work should investigate the applicability of the framework across different material systems, alternative manufacturing technologies, and production scenarios. Such comparisons would provide a more comprehensive understanding of sustainability trade-offs and further strengthen the framework's utility for sustainable manufacturing design and optimization.

Supplementary Materials: The following supporting information can be downloaded at: https://www.mdpi.com/article/10.3390/su182312142/s1, File S1: Density and crystallographic isotropy results for 154 specimens.

Author Contributions: D.M.: Conceptualization, Methodology, Investigation, Writing—Original Draft, Writing—Review and Editing, Project Administration. E.P.: Conceptualization, Methodology, Validation, Visualization, Writing—Original Draft. S.M.: Software, Validation, Formal Analysis, Investigation, Resources, Data Curation, Writing—Original Draft, Visualization. C.S.: Data Curation, Writing—Review and Editing. A.F.: Resources, Writing—Review and Editing, Supervision, Funding Acquisition. All authors have read and agreed to the published version of the manuscript.

Funding: The authors received no financial support for the research, authorship, and/or publication of this article.

Institutional Review Board Statement: Not applicable

Informed Consent Statement: Not applicable

Data Availability Statement: Data available on request due to privacy/ethical restrictions: The data that support the findings of this study are available on request from the corresponding author, [D.M.].

Conflicts of Interest: The authors declare no conflict of interest.

References

1. Frazier, W.E. Metal additive manufacturing: A review. *J. Mater. Eng. Perform.* **2014**, *23*, 1917–1928. https://doi.org/10.1007/S11665-014-0958-Z.
2. Nguyen, H.D.; Pramanik, A.; Basak, A.; Dong, Y.; Prakash, C.; Debnath, S.; Shankar, S.; Jawahir, I.; Dixit, S.; Buddhi, D. A critical review on additive manufacturing of Ti-6Al-4V alloy: Microstructure and mechanical properties. *J. Mater. Res. Technol.* **2022**, *18*, 4641–4661. https://doi.org/10.1016/j.jmrt.2022.04.055.
3. Bandyopadhyay, A.; Zhang, Y.; Bose, S. Recent developments in metal additive manufacturing. *Curr. Opin. Chem. Eng.* **2020**, *28*, 96–104. https://doi.org/10.1016/j.coche.2020.03.001.

4. Oliveira, J.P.; LaLonde, A.D.; Ma, J. Processing parameters in laser powder bed fusion metal additive manufacturing. *Mater. Des.* **2020**, *193*, 108762. https://doi.org/10.1016/j.matdes.2020.108762.
5. Gong, H.; Rafi, K.; Gu, H.; Starr, T.; Stucker, B. Analysis of defect generation in Ti–6Al–4V parts made using powder bed fusion additive manufacturing processes. *Addit. Manuf.* **2014**, *1–4*, 87–98. https://doi.org/10.1016/j.addma.2014.08.002.
6. Brenne, F.; Niendorf, T. Damage tolerant design by microstructural gradation–Influence of processing parameters and build orientation on crack growth within additively processed 316L. *Mater. Sci. Eng. A* **2019**, *764*, 138186. https://doi.org/10.1016/j.msea.2019.138186.
7. Cao, L.; Li, J.; Hu, J.; Liu, H.; Wu, Y.; Zhou, Q. Optimization of surface roughness and dimensional accuracy in LPBF additive manufacturing. *Opt. Laser Technol.* **2021**, *142*, 107246. https://doi.org/10.1016/j.optlastec.2021.107246.
8. Schwerz, C.; Schulz, F.; Natesan, E.; Nyborg, L. Increasing productivity of laser powder bed fusion manufactured Hastelloy X through modification of process parameters. *J. Manuf. Process.* **2022**, *78*, 231–241. https://doi.org/10.1016/j.jmapro.2022.04.013.
9. Sofras, C.; Čapek, J.; Li, X.; Roth, C.; Leinenbach, C.; Logé, R.; Strobl, M.; Polatidis, E. Site-specifically tailored microstructures with enhanced strength and hardening through laser powder bed fusion. *Mater. Des.* **2024**, *237*, 112539. https://doi.org/10.1016/j.matdes.2023.112539.
10. Acharya, R.; Sharon, J.A.; Staroselsky, A. Prediction of microstructure in laser powder bed fusion process. *Acta Mater.* **2017**, *124*, 360–371. https://doi.org/10.1016/j.actamat.2016.11.018.
11. Liu, Q.; Wu, H.; Paul, M.J.; He, P.; Peng, Z.; Gludovatz, B.; Kruzic, J.J.; Wang, C.H.; Li, X. Machine-learning assisted laser powder bed fusion process optimization for AlSi10Mg: New microstructure description indices and fracture mechanisms. *Acta Mater.* **2020**, *201*, 316–328. https://doi.org/10.1016/j.actamat.2020.10.010.
12. Tur, E. A Comprehensive Review on Sustainability and Environmental Impact of Laser Powder Bed Fusion Additively Manufactured As-Built Ti-6Al-4V Parts. *El-Cezeri Fen ve Mühendislik Derg.* **2023**, *10*, 612–644. https://doi.org/10.31202/ecjse.1325609.
13. Purvis, B.; Mao, Y.; Robinson, D. Three pillars of sustainability: In search of conceptual origins. *Sustain. Sci.* **2019**, *14*, 681–695. https://doi.org/10.1007/s11625-018-0627-5.
14. Giovannoni, E.; Fabietti, G. What is sustainability? A review of the concept and its applications. In *Integrated Reporting: Concepts and Cases that Redefine Corporate Accountability*; Springer: Cham, Switzerland, 2013; pp. 21–40. https://doi.org/10.1007/978-3-319-02168-3_2.
15. Benedetti, M.; Perini, M.; Vanazzi, M.; Giorgini, A.; Macoretta, G.; Menapace, C. Atomized scrap powder feedstock for sustainable Inconel 718 additive manufacturing via LPBF: A study of static and fatigue properties. *Prog. Addit. Manuf.* **2023**, *9*, 1843–1856. https://doi.org/10.1007/s40964-023-00547-z. Correction in *Prog. Addit. Manuf.* **2025**, *10*, 3065. https://doi.org/10.1007/s40964-024-00872-x.
16. Wurst, J.; Mozgova, I.; Lachmayer, R. Sustainability Assessment of Products manufactured by the Laser Powder Bed Fusion (LPBF) Process. *Procedia CIRP* **2022**, *105*, 243–248. https://doi.org/10.1016/j.procir.2022.02.040.
17. Mecheter, A.; Tarlochan, F.; Kucukvar, M. A Review of Conventional versus Additive Manufacturing for Metals: Life-Cycle Environmental and Economic Analysis. *Sustainability* **2023**, *15*, 12299. https://doi.org/10.3390/su151612299.
18. Raoufi, K.; Haapala, K.R.; Etheridge, T.; Manoharan, S.; Paul, B.K. Cost and environmental impact assessment of stainless steel microscale chemical reactor components using conventional and additive manufacturing processes. *J. Manuf. Syst.* **2022**, *62*, 202–217. https://doi.org/10.1016/j.jmsy.2021.11.017.
19. Liao, J.; De Kleine, R.; Kim, H.C.; Luckey, G.; Forsmark, J.; Lee, E.C.; Cooper, D.R. Assessing the sustainability of laser powder bed fusion and traditional manufacturing processes using a parametric environmental impact model. *Resour. Conserv. Recycl.* **2023**, *198*, 107138. https://doi.org/10.1016/j.resconrec.2023.107138.
20. Sabzi, H.E.; Rivera-Díaz-Del-Castillo, P.E.J. Sustainable Powder-Based Additive Manufacturing Technology. *Sustainability* **2023**, *15*, 15081. https://doi.org/10.3390/su152015081.
21. Pesode, P.; Barve, S. Additive manufacturing of metallic biomaterials: Sustainability aspect, opportunity, and challenges. *J. Ind. Prod. Eng.* **2023**, *40*, 464–505. https://doi.org/10.1080/21681015.2023.2229341.
22. Manco, P.; Caterino, M.; Rinaldi, M.; Macchiaroli, R. A sustainability-oriented methodology to compare production strategies: The case of AM-based remanufacturing. *J. Clean. Prod.* **2023**, *423*, 138594. https://doi.org/10.1016/j.jclepro.2023.138594.
23. Chandra, M.; Shahab, F.; Kek, V.; Rajak, S. Selection for additive manufacturing using hybrid MCDM technique considering sustainable concepts. *Rapid Prototyp. J.* **2022**, *28*, 1297–1311. https://doi.org/10.1108/rpj-06-2021-0155.
24. Palanisamy, M.; Pugalendhi, A.; Ranganathan, R. Selection of suitable additive manufacturing machine and materials through best–worst method (BWM). *Int. J. Adv. Manuf. Technol.* **2020**, *107*, 2345–2362. https://doi.org/10.1007/s00170-020-05110-6.

25. Raigar, J.; Sharma, V.S.; Srivastava, S.; Chand, R.; Singh, J. A decision support system for the selection of an additive manufacturing process using a new hybrid MCDM technique. *Sādhanā* **2020**, *45*, 1–14. https://doi.org/10.1007/s12046-020-01338-w.
26. Mercurio, V.; Calignano, F.; Iuliano, L. Sustainable production of AlSi10Mg parts by laser powder bed fusion process. *Int. J. Adv. Manuf. Technol.* **2023**, *125*, 3117–3133. https://doi.org/10.1007/s00170-023-11004-0. Correction in *Int. J. Adv. Manuf. Technol.* **2024**, *130*, 3149. https://doi.org/10.1007/s00170-023-12883-z.
27. Nyamekye, P.; Lakshmanan, R.; Tepponen, V.; Westman, S. Sustainability aspects of additive manufacturing: Leveraging resource efficiency via product design optimization and laser powder bed fusion. *Heliyon* **2023**, *10*, e23152. https://doi.org/10.1016/j.heliyon.2023.e23152.
28. Khaimovich, A.; Balyakin, A.; Oleynik, M.; Meshkov, A.; Smelov, V. Optimization of Process Parameters for Powder Bed Fusion Additive Manufacturing Using a Linear Programming Method: A Conceptual Framework. *Metals* **2022**, *12*, 1976. https://doi.org/10.3390/met12111976.
29. Gruber, K.; Smolina, I.; Kasprowicz, M.; Kurzynowski, T. Evaluation of Inconel 718 Metallic Powder to Optimize the Reuse of Powder and to Improve the Performance and Sustainability of the Laser Powder Bed Fusion (LPBF) Process. *Materials* **2021**, *14*, 1538. https://doi.org/10.3390/ma14061538.
30. Vilanova, M.; Escribano-García, R.; Guraya, T.; Sebastian, M.S. Optimizing laser powder bed fusion parameters for IN-738LC by response surface method. *Materials* **2020**, *13*, 4879. https://doi.org/10.3390/ma13214879.
31. Hoschke, K.; Kappe, K.; Patil, S.; Kilchert, S.; Kim, J.; Pfaff, A. Sustainability-Oriented Topology Optimization Towards a More Holistic Design for Additive Manufacturing. In *Springer Tracts in Additive Manufacturing*; Springer: Cham, Switzerland, 2024; Volume Part F3256, pp. 77–88. https://doi.org/10.1007/978-3-031-42983-5_6.
32. Dimopoulos, A.; Zournatzis, I.; Gan, T.-H.; Chatzakos, P. Multi-Response Optimization of Ti6Al4V Support Structures for Laser Powder Bed Fusion Systems. *J. Manuf. Mater. Process.* **2023**, *7*, 22. https://doi.org/10.3390/jmmp7010022. Correction *in J. Manuf. Mater. Process.* **2023**, *7*, 85. https://doi.org/10.3390/jmmp7030085.
33. La Fé-Perdomo, I.; Ramos-Grez, J.A.; Jeria, I.; Guerra, C.; Zambrano-Robledo, P. Simultaneous Optimization of Surface Roughness and Mechanical Properties of 316L Produced by LB–PBF Using Grey Relational Analysis Complemented by Residual Stress Analysis. *Arab. J. Sci. Eng.* **2024**, *49*, 2285–2298. https://doi.org/10.1007/s13369-023-08215-8.
34. Sofras, C.; Čapek, J.; Leinenbach, C.; Logé, R.E.; Strobl, M.; Polatidis, E. Exploring crystallographic texture manipulation in stainless steels via laser powder bed fusion: Insights from neutron diffraction and machine learning. *Virtual Phys. Prototyp.* **2024**, *19*, e2390483. https://doi.org/10.1080/17452759.2024.2390483.
35. Sofras, C.; Čapek, J.; Leinenbach, C.; Logé, R.E.; Strobl, M.; Polatidis, E. Supplementary material for: Exploring crystallographic texture manipulation in stainless steels via laser powder bed fusion: Insights from neutron diffraction and machine learning. *Zenodo* **2024**. https://doi.org/10.5281/zenodo.11189615.
36. Markatos, D.N.; Katsiropoulos, C.V.; Tserpes, K.I.; Pantelakis, S.G. A holistic End-of-Life (EoL) Index for the quantitative impact assessment of CFRP waste recycling techniques. *Manuf. Rev.* **2021**, *8*, 18. https://doi.org/10.1051/mfreview/2021016.
37. Malefaki, S.; Markatos, D.; Filippatos, A.; Pantelakis, S. A Comparative Analysis of Multi-Criteria Decision-Making Methods and Normalization Techniques in Holistic Sustainability Assessment for Engineering Applications. *Aerospace* **2025**, *12*, 100. https://doi.org/10.3390/aerospace12020100.
38. Saaty, T.L. "Analytic Hierarchy Process Planning, Priority Setting, Resource Allocation." Advanced Optimization and Decision-Making Techniques in Textile Manufacturing. 1980; p. 287. Available online: https://books.google.com/books/about/The_Analytic_Hierarchy_Process.html?hl=el&id=Xxi7AAAAIAAJ (accessed on 16 November 2024).
39. Rodrigues, G.C.; Cuypers, M.; Sichani, E.F.; Kellens, K.; Duflou, J. Laser cutting with direct diode laser. *Phys. Procedia* **2013**, *41*, 558–565. https://doi.org/10.1016/j.phpro.2013.03.116.
40. Breiman, L.; Friedman, J.H.; Olshen, R.A.; Stone, C.J. *Classification and Regression Trees*; Chapman & Hall/CRC: Boca Raton, FL, USA, 2017; pp. 1–358. https://doi.org/10.1201/9781315139470
41. Vaish, R.; Dwivedi, U.; Tewari, S.; Tripathi, S. Machine learning applications in power system fault diagnosis: Research advancements and perspectives. *Eng. Appl. Artif. Intell.* **2021**, *106*, 104504. https://doi.org/10.1016/j.engappai.2021.104504.
42. DebRoy, T.; Wei, H.L.; Zuback, J.S.; Mukherjee, T.; Elmer, J.W.; Milewski, J.O.; Beese, A.M.; Wilson-Heid, A.; De, A.; Zhang, W. Additive manufacturing of metallic components–Process, structure and properties. *Prog. Mater. Sci.* **2018**, *92*, 112–224. https://doi.org/10.1016/j.pmatsci.2017.10.001.
43. Bertoli, U.S.; Wolfer, A.J.; Matthews, M.J.; Delplanque, J.-P.R.; Schoenung, J.M. On the limitations of Volumetric Energy Density as a design parameter for Selective Laser Melting. *Mater. Des.* **2017**, *113*, 331–340. https://doi.org/10.1016/j.matdes.2016.10.037.

44. R Core Team. *R: A Language and Environment for Statistical Computing*; R Foundation for Statistical Computing: Vienna, Austria, 2018. Available online: https://www.gbif.org/tool/81287/r-a-language-and-environment-for-statistical-computing (accessed on 15 October 2021).
45. Therneau, T.; Atkinson, B. *Recursive Partitioning and Regression Trees (R Package rpart Version 4.1.23)*; Comprehensive R Archive Network (CRAN): Vienna, Austria, 2023. https://doi.org/10.32614/CRAN.PACKAGE.RPART.
46. United Nations Environment Programme (UNEP). *Guidelines for Social Life Cycle Assessment of Products and Organizations 2020*; UNEP: Nairobi, Kenya, 2020
47. Ashby, M.; Vakhitova, T.; Vallejo-Olivares, A. Social Life Cycle Assessment and Social Impact Audit Tool. Available online: https://www.researchgate.net/publication/336346723 (accessed on 26 November 2024).
48. 2024_07_international_electricity_factors_1.xlsx. Available online: https://view.officeapps.live.com/op/view.aspx?src=https%3A%2F%2Fwww.carbonfootprint.com%2Fdocs%2F2024_07_international_electricity_factors_1.xlsx&wdOrigin=BROWSELINK (accessed on 26 November 2024).
49. China: Business Electricity Prices 2024|Statista. Available online: https://www.statista.com/statistics/1373596/business-electricity-price-china/ (accessed on 14 November 2024).
50. U.S.: Industrial Electricity Prices Monthly 2024|Statista. Available online: https://www.statista.com/statistics/1395805/monthly-electricity-price-industrial-sector-united-states/ (accessed on 14 November 2024).
51. Statistics|Eurostat. Available online: https://ec.europa.eu/eurostat/databrowser/view/ten00117/default/map?lang=en (accessed on 14 November 2024).
52. Natural Resources Canada. *Energy Fact Book 2025–2026*. Government of Canada, Ottawa, Canada, 2025. Available online: https://energy-information.canada.ca/sites/default/files/2025-11/energy-fact-book-2025-2026.pdf (accessed on 22 November 2026).
53. International Electricity Prices: How Does Australia Compare? Available online: https://www.energycouncil.com.au/analysis/international-electricity-prices-how-does-australia-compare/ (accessed on 14 November 2024).
54. United Arab Emirates Electricity Prices, March 2024|GlobalPetrolPrices.com. Available online: https://www.globalpetrolprices.com/United-Arab-Emirates/electricity_prices/ (accessed on 14 November 2024).
55. Statistics|Eurostat. Available online: https://ec.europa.eu/eurostat/databrowser/view/nrg_pc_205_c/default/table?lang=en (accessed on 14 November 2024).
56. Czech Republic–Electricity Prices: Non-Household, Medium Size Consumers–2024 Data 2025 Forecast 2010 Historical. Available online: https://tradingeconomics.com/czech-republic/electricity-prices-non-household-medium-size-consumers-eurostat-data.html (accessed on 14 November 2024).
57. Average Salary in Dubai per Month, UAE–Flowace.ai. Available online: https://flowace.ai/blog/average-salary-in-dubai-per-month/ (accessed on 13 November 2024).
58. Manufacturing Labor Costs per Hour: China, Vietnam, Mexico 2016–2020|Statista. Available online: https://www.statista.com/statistics/744071/manufacturing-labor-costs-per-hour-china-vietnam-mexico/ (accessed on 13 November 2024).
59. Statistics on Labour Costs–ILOSTAT. Available online: https://ilostat.ilo.org/topics/labour-costs/ (accessed on 13 November 2024).
60. Vallejo, N.D.; Lucas, C.; Ayers, N.; Graydon, K.; Hyer, H.; Sohn, Y. Process Optimization and Microstructure Analysis to Understand Laser Powder Bed Fusion of 316L Stainless Steel. *Metals* **2021**, *11*, 832. https://doi.org/10.3390/met11050832.
61. Evangelou, A.; Stylianou, R.; Loizou, A.; Kim, D.; Liang, A.; Reed, P.; Constantinides, G.; Kyratsi, T. Effects of process parameters and scan strategy on the microstructure and density of stainless steel 316L produced via laser powder bed fusion. *J. Alloys Metall. Syst.* **2023**, *3*, 100027. https://doi.org/10.1016/j.jalmes.2023.100027.
62. Rizk, N.; Nazzal, M.; Darras, B.M.; Deiab, I. Comparative sustainability assessment of laser powder bed fusion additive manufacturing and conventional machining for Ti-6Al-4V: A multi-criteria decision-making approach. *J. Clean. Prod.* **2025**, *525*, 146569. https://doi.org/10.1016/j.jclepro.2025.146569.

Disclaimer/Publisher's Note: The statements, opinions and data contained in all publications are solely those of the individual author(s) and contributor(s) and not of MDPI and/or the editor(s). MDPI and/or the editor(s) disclaim responsibility for any injury to people or property resulting from any ideas, methods, instructions or products referred to in the content.